

WW + jet at 14 and 100 TeV

John Campbell

Fermilab

E-mail: johnmc@fnal.gov

David Miller

University of Glasgow

E-mail: david.j.miller@glasgow.ac.uk

Tania Robens*

IKTP, TU Dresden

E-mail: tania.robens@tu-dresden.de

In the current LHC run, an accurate understanding of Standard Model processes is extremely important. Processes including electroweak gauge bosons serve as standard candles for SM measurements, and equally constitute important backgrounds for Beyond-the-Standard Model (BSM) searches. We present here the next-to-leading order (NLO) QCD virtual contributions to $W^+W^- + \text{jet}$ in an analytic format obtained through unitarity methods. We present results for the full process using the Monte Carlo event generator MCFM, and discuss total as well as differential cross-sections for the LHC with 14 TeV center-of-mass energy, as well as a future 100 TeV proton-proton machine.

FERMILAB-CONF-16-514-T

38th International Conference on High Energy Physics

3-10 August 2016

Chicago, USA

*Speaker.

1. Overview

We consider the hadronic production of W pairs in association with a single jet at next-to-leading order (NLO) in QCD at a hadron collider with a center-of-mass energy of 14 and 100 TeV. The W bosons decay leptonically, with all spin correlations included. At tree level this process corresponds to the partonic reaction,

$$q + \bar{q} \rightarrow W^+ + W^- + g \quad (1.1)$$

$$\begin{array}{l} \phantom{q + \bar{q} \rightarrow W^+ + W^- + g} \quad \quad \quad \downarrow \\ \phantom{q + \bar{q} \rightarrow W^+ + W^- + g} \quad \quad \quad \mu^- + \nu_\mu \\ \phantom{q + \bar{q} \rightarrow W^+ + W^- + g} \quad \quad \quad \downarrow \\ \phantom{q + \bar{q} \rightarrow W^+ + W^- + g} \quad \quad \quad \nu_e + e^+ \end{array}$$

with all possible crossings of the partons between initial and final states. Here, the W bosons can either be radiated off a quark line or mediated via an offshell Z -boson that decays into a W^+W^- pair. Next-to-leading order contributions include the emission of an additional parton, either as a virtual particle to form a loop amplitude, or as a real external particle (cf. Fig. 1). All results presented here have been obtained using Ref. [1], where we made use of the methods of generalized unitarity [2, 3, 4, 5, 6, 7], furthermore employing the S@M Mathematica package [8] for the analytic treatment and simplification. The evaluation of the scalar integrals has been performed using the QCDLoop Fortran library [9]. The combination of the virtual contributions with born and real emission diagrams has been implemented using MCFM [10, 11], and applied in a recent analysis by the ATLAS collaboration [12]. Note that we do not include the effects of any third-generation quarks.

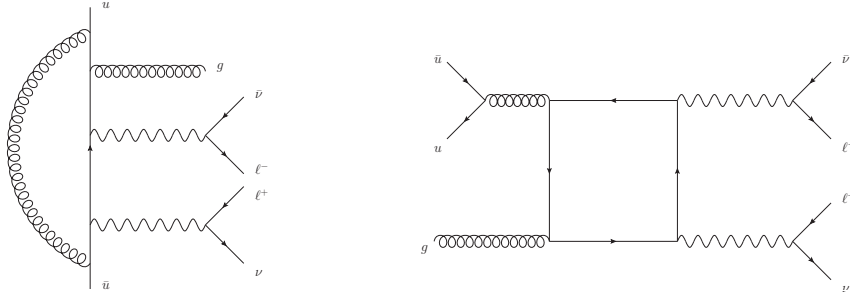


Figure 1: Sample diagrams entering the calculation of the one-loop amplitude for the WW +jet process. The one-loop diagrams can be categorized according to whether a gluon dresses a leading-order amplitude (left), or whether the diagram includes a closed fermion loop (right).

2. Analytic and numerical results

Explicit expressions for sample coefficients have been presented in detail in [1, 13] and will not be repeated here. Instead, we choose to discuss results specific for a proton-proton collider with a center-of-mass energy of 100 TeV (see also [14]). Electroweak parameters as given in Tab. 1 were used for all results presented here. In calculations of LO quantities we employ the CTEQ6L1 PDF set [15], while at NLO we use CT10 [16]. The renormalization and factorization scales are usually

m_W	80.385 GeV	Γ_W	2.085 GeV
m_Z	91.1876 GeV	Γ_Z	2.4952 GeV
e^2	0.095032	g_W^2	0.42635
$\sin^2 \theta_W$	0.22290	G_F	0.116638×10^{-4}

Table 1: The values of the mass, width and electroweak parameters used.

chosen to be the same, $\mu_R = \mu_F = \mu$, with our default scale choice $\mu_0 \equiv \frac{H_T}{2} = \frac{1}{2} \sum_i p_{\perp}^i$. The sum over the index i runs over all final state leptons and partons. Jets are defined using the anti- k_T algorithm with separation parameter $R = 0.5$ and must satisfy $p_{\perp}^{\text{jet}} > p_{\perp, \text{cut}}^{\text{jet}}$, $|\eta^{\text{jet}}| < 4.5$.

Total cross-sections predicted at LO and NLO are shown in Fig. 2, as a function of $p_{\perp, \text{cut}}^{\text{jet}}$ and for values as large as 400 GeV at the 100 TeV machine. All numbers cited in this section do not take into account the decays of the W bosons, and branching ratios must be applied accordingly. The theoretical uncertainty band is computed by using a series of scale variations, cf. [1, 13]. The cross-sections at NLO are significantly larger than those at LO and, in general, the uncertainty bands do not overlap. At 100 TeV the cross-sections are about an order of magnitude larger than at 14 TeV. For the case of a 100 TeV collider, we see that p_{\perp}^{jet} -cuts of $\mathcal{O}(10 \text{ TeV})$ or higher still render measurable cross-sections, at least for a high-luminosity scenario, cf. Fig. 3. Similar results are obtained for total cross-sections with an additional cut on either $H_T^{\text{jets}} = \sum_{\text{jets}} p_{\perp}^{\text{jet}}$ or $|p_T^{WW}| \equiv |p_T^{\text{jets}}|$, the transverse momentum of the *complete* jet system, cf. Fig. 4; in both cases, $p_{\perp, \text{cut}}^{\text{jet}} = 25 \text{ GeV}$. In case of the p_{\perp} cut on the total jet system (or, equivalently, the WW system), K-factors of 2 – 3 prevail up to cut values $\lesssim 16 \text{ TeV}$.

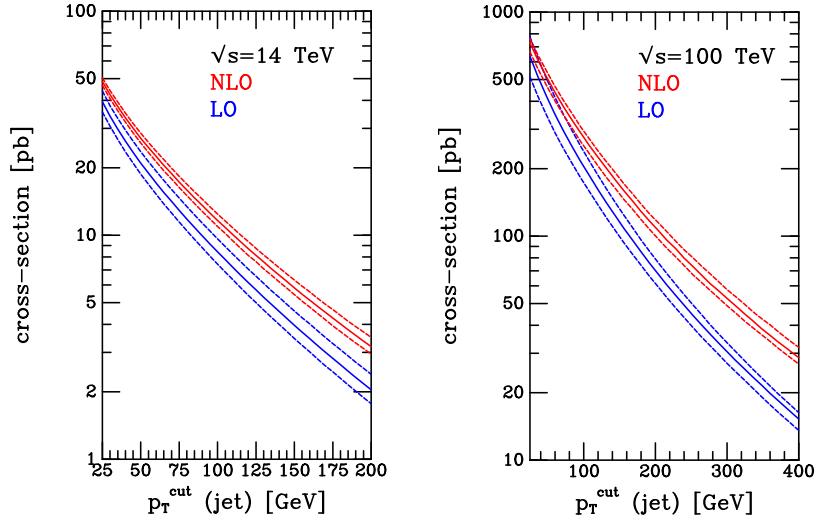


Figure 2: Cross-sections at $\sqrt{s} = 14 \text{ TeV}$ (left) and 100 TeV (right), as a function of the transverse momentum cut on the jet. The prediction at each order is shown as a solid line, with the dotted lines indicating the scale uncertainty corresponding to a factor of two variation about the central scale.

Regarding differential distributions, we briefly comment on an observable that is particularly interesting for Higgs searches at colliders, i.e. the azimuthal angle between the electron and the

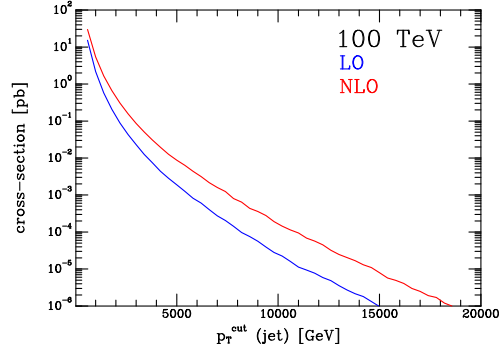


Figure 3: Cross-sections at 100 TeV, as a function of the transverse momentum cut on the jet.

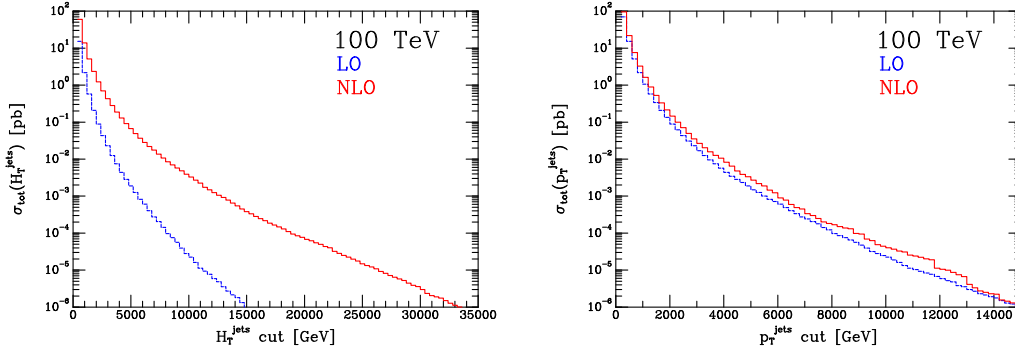


Figure 4: Total integrated cross-sections at LO and NLO, with additional lower cuts on $H_T^{\text{jets}} = \sum_{\text{jets}} p_{\perp}^{\text{jet}}$ (left) and $|p_T^{WW}| \equiv |p_T^{\text{jets}}|$. See main body of text for details.

\sqrt{s}	$p_{\perp, \text{cut}}^{\text{jet}}$	σ_{LO} [pb]	σ_{NLO} [pb]
14 TeV	25 GeV	$39.5^{+11.7\%}_{-11.0\%}$	$48.6^{+3.8\%}_{-4.0\%}$
100 TeV	25 GeV	$648^{+22.3\%}_{-19.3\%}$	$740^{+4.5\%}_{-9.3\%}$
100 TeV	300 GeV	$30.3^{+11.22\%}_{-10.56\%}$	$53.7^{+8.0\%}_{-7.6\%}$

Table 2: Cross-sections for the process $pp \rightarrow WW + \text{jet}$ at proton-proton colliders of various energies, together with estimates of the theoretical uncertainty from scale variation as described in the text. Monte Carlo uncertainties are at most a single unit in the last digit shown in the table.

positron, which can be used to isolate contributions to this final state from Higgs boson decays. We here compare differential distributions at the 14 TeV LHC as well as a 100 TeV collider, normalized by the respective total cross-section; in the latter case, we now additionally consider a scenario where the minimal p_{\perp} cut on the jet has been set to 300 GeV. Production cross-sections for these cases are given in Tab. 2. As shown in Fig. 5, under the usual jet cuts at 14 TeV, this distribution is peaked towards $\Delta\Phi_{\ell\ell} = \pi$, a feature which persists at 100 TeV using the same jet cut. Once the jet cut is raised significantly, the recoil of the W^+W^- system results in the two leptons instead being preferentially produced closer together, i.e. in the region $\Delta\Phi_{\ell\ell} \rightarrow 0$; this region is usually

favoured by events resulting from Higgs mediation. Even if the jet threshold at a 100 TeV collider were not as high as 300 GeV, such a shift in this distribution could be an important consideration in optimizing the according analyses in this channel. On the other hand, the $m_{\ell\ell}$ distribution remains similar, albeit with a longer tail in the high-energy scenario.

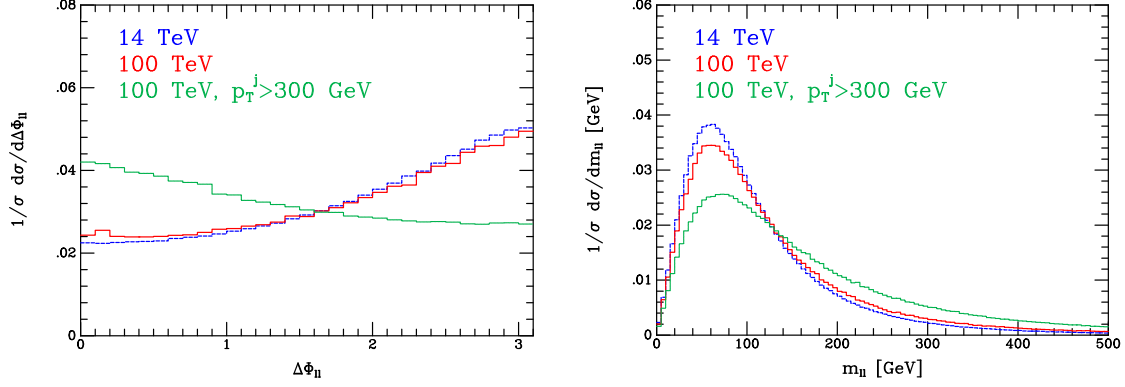


Figure 5: NLO $\Delta\Phi_{\ell\ell}$ (left) and $m_{\ell\ell}$ (right) distributions, normalized by the respective total cross-sections, for 14 TeV (red), 100 TeV (blue), and 100 TeV with an increased p_{\perp}^{jet} cut (green)

3. Summary

In the current run of the LHC, precise knowledge of predictions for SM processes is more crucial than ever. We have considered the process $W^+W^- + \text{jet}$ at NLO QCD, making use of an analytic calculation implemented into MCFM. We have considered total cross-sections as well as differential distributions at proton-proton colliders with 14 TeV and 100 TeV center-of-mass energies for various cut scenarios. We found that in general at 100 TeV dimensionful variables such as $m_{\ell\ell}$ exhibit longer tails in the distributions, reflecting the increased center-of-mass energy of the system. Furthermore, applying a higher p_{\perp} cut significantly changes distributions for the dilepton azimuthal angle $\Delta\Phi_{\ell\ell}$, frequently used for background suppression for Higgs measurements.

Acknowledgements

T.R. would like to thank the Fermilab Theory Group for their repeated hospitality while this work was completed. DJM is supported by the UK Science and Technology Facilities Council (STFC) under grant ST/L000446/1. This research is supported by the US DOE under contract DE-AC02-07CH11359.

References

[1] John M. Campbell, David J. Miller, and Tania Robens. Next-to-Leading Order Predictions for WW+Jet Production. *Phys. Rev.*, D92(1):014033, 2015, 1506.04801.

- [2] Ruth Britto, Freddy Cachazo, and Bo Feng. Generalized unitarity and one-loop amplitudes in N=4 super-Yang-Mills. *Nucl.Phys.*, B725:275–305, 2005, hep-th/0412103.
- [3] Ruth Britto, Evgeny Buchbinder, Freddy Cachazo, and Bo Feng. One-loop amplitudes of gluons in SQCD. *Phys.Rev.*, D72:065012, 2005, hep-ph/0503132.
- [4] Ruth Britto, Bo Feng, and Pierpaolo Mastrolia. The Cut-constructible part of QCD amplitudes. *Phys.Rev.*, D73:105004, 2006, hep-ph/0602178.
- [5] Darren Forde. Direct extraction of one-loop integral coefficients. *Phys.Rev.*, D75:125019, 2007, 0704.1835.
- [6] Pierpaolo Mastrolia. Double-Cut of Scattering Amplitudes and Stokes’ Theorem. *Phys.Lett.*, B678:246–249, 2009, 0905.2909.
- [7] S.D. Badger. Direct Extraction Of One Loop Rational Terms. *JHEP*, 0901:049, 2009, 0806.4600.
- [8] D. Maitre and P. Mastrolia. S@M, a Mathematica Implementation of the Spinor-Helicity Formalism. *Comput.Phys.Commun.*, 179:501–574, 2008, 0710.5559.
- [9] R. Keith Ellis and Giulia Zanderighi. Scalar one-loop integrals for QCD. *JHEP*, 0802:002, 2008, 0712.1851.
- [10] John M. Campbell and R. Keith Ellis. An Update on vector boson pair production at hadron colliders. *Phys.Rev.*, D60:113006, 1999, hep-ph/9905386.
- [11] John M. Campbell, R. Keith Ellis, and Walter T. Giele. A Multi-Threaded Version of MCFM. *Eur.Phys.J.*, C75(6):246, 2015, 1503.06182.
- [12] Morad Aaboud et al. Measurement of W^+W^- production in association with one jet in proton–proton collisions at $\sqrt{s} = 8$ TeV with the ATLAS detector. *Phys. Lett.*, B763:114–133, 2016, 1608.03086.
- [13] John Campbell, David Miller, and Tania Robens. $W^+W^- + \text{Jet}$: Compact Analytic Results. In *Proceedings, 12th International Symposium on Radiative Corrections (Radcor 2015) and LoopFest XIV (Radiative Corrections for the LHC and Future Colliders): Los Angeles, CA, USA, June 15-19, 2015*, 2016, 1601.03563.
- [14] M. L. Mangano et al. Physics at a 100 TeV pp collider: Standard Model processes. 2016, 1607.01831.
- [15] J. Pumplin, D.R. Stump, J. Huston, H.L. Lai, Pavel M. Nadolsky, et al. New generation of parton distributions with uncertainties from global QCD analysis. *JHEP*, 0207:012, 2002, hep-ph/0201195.
- [16] Hung-Liang Lai, Marco Guzzi, Joey Huston, Zhao Li, Pavel M. Nadolsky, et al. New parton distributions for collider physics. *Phys.Rev.*, D82:074024, 2010, 1007.2241.